Supplementary Information

for

Charge distribution and conformational stability effects of organic structure-directing agents on zeolite synthesis

Donghui Jo and Suk Bong Hong*

Center for Ordered Nanoporous Materials Synthesis, Division of Environmental Science and Engineering, POSTECH, Pohang 37673, Korea

*sbhong@postech.ac.kr

Experimental Details

Organic Structure-Directing Agent (OSDA) Synthesis. A general procedure for the alkylation of pyrazole derivatives: a mixture of 0.200 mol pyrazole (95-98%, Bepharm) and 0.400 mol alkyl iodide (99%, Aldrich) was refluxed in 100 mL acetonitrile (99.9%, Samchun) for 4 days. (Caution: This reaction can be highly exothermic and make the mixture acidic, use appropriate precautions.) The solvent and remaining alkylation agent were removed using rotary evaporation at 90 °C (Caution: Toxic vapors may evolve, use appropriate precautions), and the product was washed by ethyl acetate (99.5%, Samchun).

1,2,3-trimethylpyrazolium (123TMP) iodide: 1,5-dimethylpyrazole and iodomethane were used as reactants. ^{1}H NMR (300 MHz, D_2O): δ 2.36 (s, 3H), 3.84 (s, 3H), 3.96 (s, 3H), 6.46 (d, 1H), 7.90 (d, 1H). ^{13}C NMR (75 MHz, D_2O): δ 13.2, 34.8, 38.4, 108.8, 138.0, 149.0

1,2,4-trimethylpyrazolium (124TMP) iodide: 1,4-methylpyrazole and iodomethane were used as reactants. ^{1}H NMR (300 MHz, D_2O): δ 2.00 (s, 3H), 3.92 (s, 2H), 7.81 (s, 6H). ^{13}C NMR (75 MHz, D_2O): δ 9.6, 38.0, 119.7, 138.2.

1,2,3,5-tetramethylpyrazolium (1235TMP) iodide: 1,3,5-trimethylpyrazole and iodomethane were used as reactants. ^{1}H NMR (300 MHz, D_2O): δ 2.31 (s, 6H), 3.80 (s, 6H), 6.30 (s, 1H). ^{13}C NMR (75 MHz, D_2O): δ 11.1, 33.1, 107.0, 145.8.

1-ethyl-2,3-dimethylpyrazolium (1E23DMP) iodide: 1,5-dimethylpyrazole and iodoethane were used as reactants. ^{1}H NMR (300 MHz, D_2O): δ 1.42 (t, 3H), 2.36 (s, 3H), 3.85 (s, 3H), 4.31 (q, 2H), 6.47 (d, 1H), 7.95 (d, 1H). ^{13}C NMR (75 MHz, D_2O): δ 13.3, 15.1, 35.0, 47.2, 109.0, 136.4, 149.3.

1-ethyl-2,5-dimethylpyrazolium (1E25DMP) iodide: 1,3-dimethylpyrazole and iodoethane were used as reactants. ^{1}H NMR (300 MHz, D_2O): δ 1.31 (t, 3H), 2.39 (s, 3H), 3.99 (s, 3H), 4.34 (q, 2H), 6.46 (d, 1H), 7.90 (d, 1H). ^{13}C NMR (75 MHz, D_2O): δ 13.1, 15.1, 38.6, 43.9, 109.2, 138.7, 148.6.

1-ethyl-2,3,5-trimethylpyrazolium (1E235TMP) iodide: 1,3,5-trimethylpyrazole and iodoethane were used as reactants. ^{1}H NMR (300 MHz, D_2O): δ 1.27 (t, 3H), 2.29 (s, 3H), 2.32 (s, 3H), 3.81 (s, 3H), 4.28 (q, 2H), 6.28 (s, 1H). ^{13}C NMR (75 MHz, D_2O): δ 12.8, 13.1, 15.3, 35.2, 43.9, 109.4, 147.3, 148.3

Six imidazolium derivatives employed in this work were also prepared according to the procedures described in the literature.[S1,S2] Prior to its use as an OSDA, the halide salt of each of diazolium cations obtained was converted to the hydroxide form by anion exchange in aqueous solution using Amberlite IRN-78 anion-exchange resin (Aldrich). Then, the resulting

solution was concentrated by rotary evaporation at 80 °C, and its final hydroxide concentration was determined by titration using phenolphthalein as an indicator.

Zeolite Synthesis. The synthesis of pure-silica zeolites in the presence of imidazolium- or pyrazolium-based OSDAs was performed using synthesis mixtures prepared by combining HF (48%, J.T.Baker), tetraethylorthosilicate (TEOS, 98%, Aldrich), and deionized water. The composition of the final synthesis mixture was $0.50ROH \cdot 0.50HF \cdot 1.0SiO_2 \cdot xH_2O$, where R is the imidazolium or pyrazolium OSDA prepared here and x = 5.0 or 15.0. In a typical synthesis, TEOS was mixed with an appropriate amount of water in a solution of ROH and stirred at room temperature for 3 h. The resulting solution was heated at 80 °C to remove ethanol molecules generated by the hydrolysis of TEOS and some water for the desired composition. Finally, HF (48%, J.T. Baker) was added while the mixture was stirred with a spatula. The final synthesis mixture was charged into Teflon-lined 23-mL autoclaves and heated under rotation (60 rpm) at 125 or 175 °C for the desired time. The solid product was recovered by filtration or centrifugation, washed repeatedly with water, and dried overnight at room temperature.

Characterization. Powder X-ray diffraction (XRD) patterns were recorded on a PANalytical X´Pert diffractometer (Cu K_α radiation) with an X´Celerator detector. The C, H, and N contents of the samples were analyzed by using a Vario EL III elemental organic analyzer. Thermogravimetric (TGA) and differential thermal analyses (DTA) were performed in air on an SII EXSTAR 6000 thermal analyzer, where the weight losses related to the combustion of OSDAs. ^{1}H and ^{13}C solution NMR measurements for OSDA were carried out in 5 mm quartz tubes using a Bruker AVANCE III 300 spectrometer. The ^{1}H NMR spectra were recorded at a ^{1}H frequency of 300.13 MHz with a $\pi/2$ rad pulse length of 11.0 ms and a recycle delay of 2.0 s. The ^{13}C NMR spectra were recorded at a ^{13}C frequency of 75.475 MHz with a $\pi/2$ rad pulse length of 10.2 ms and a recycle delay of 1.5 s. The ^{1}H-^{13}C CP MAS NMR spectra at a spinning rate of 21 kHz were recorded on a Bruker 500 Ultrashield spectrometer at a ^{13}C frequency of 125.783 MHz with a $\pi/2$ rad pulse length of 4.8 μs, a contact time of 2.0 ms, a recycle delay of 5.0 s, and an acquisition of *ca.* 15000 pulse transients. The ^{13}C chemical shift is reported relative to TMS.

Computational Details

DFT Calculations. The geometry of OSDAs employed was optimized at the B3LYP/6-31+G(d,p) level of theory[S3] using the Gaussian 09 software package[S4] and their electrostatic potential (ESP) surface was visualized using the same program, while setting the total net molecular charge to +1. In addition, the potential energy surface (PES) scan of each OSDA about the $E_{Ar}(1)$-$E_{Ar}(2)$-$C_{Et}(3)$-$C_{Et}(4)$ torsion angle, where E is C or N (Fig. 2, S5 and S6), was carried out with a step size of 5º at the same level of theory using the Gaussian 09 program.

Molecular Mechanics Calculations. Prior to measuring the height of internal cavity or cage, the crystallographic data of four pure-silica zeolite structures (ITW, STW, NON, and MTF), downloaded from the Database of Zeolite Structures,[S5] were optimized under the constant pressure conditions with *P*1 symmetry using the Sanders-Leslie-Catlow (SLC) potential[S6] in the GULP program.[S7] The OSDA molecules were also introduced at one molecule per cavity into some zeolite structures (Table S3) and optimized using the Dreiding potential[S8] in the GULP program. The host zeolite was held fixed during the simulation.

References

S1 A. Rojas, M. L. San-Roman, C. M. Zicovich-Wilson and M. A. Camblor, *Chem. Mater.*, 2013, **25**, 729.

S2 J. E. Schmidt, M. A. Deimund, D. Xie and M. E. Davis, *Chem. Mater.*, 2015, **27**, 3756.

S3 A. D. Becke, *J. Chem. Phys.*, 1993, **98**, 5648.

S4 M. J. Frisch, G. W. Trucks, H. B. Schlegel, G. E. Scuseria, M. A. Robb, J. R. Cheeseman, G. Scalmani, V. Barone, B. Mennucci, G. A. Petersson, H. Nakatsuji, M. Caricato, X. Li, H. P. Hratchian, A. F. Izmaylov, J. Bloino, G. Zheng, J. L. Sonnenberg, M. Hada, M. Ehara, K. Toyota, R. Fukuda, J. Hasegawa, M. Ishida, T. Nakajima, Y. Honda, O. Kitao, H. Nakai, T. Vreven, J. A. Montgomery, Jr., J. E. Peralta, F. Ogliaro, M. Bearpark, J. J. Heyd, E. Brothers, K. N. Kudin, V. N. Staroverov, T. Keith, R. Kobayashi, J. Normand, K. Raghavachari, A. Rendell, J. C. Burant, S. S. Iyengar, J. Tomasi, M. Cossi, N. Rega, J. M. Millam, M. Klene, J. E. Knox, J. B. Cross, V. Bakken, C. Adamo, J. Jaramillo, R. Gomperts, R. E. Stratmann, O. Yazyev, A. J. Austin, R. Cammi, C. Pomelli, J. W. Ochterski, R. L. Martin, K. Morokuma, V. G. Zakrzewski, G. A. Voth, P. Salvador, J. J. Dannenberg, S. Dapprich, A. D. Daniels, O. Farkas, J. B. Foresman, J. V. Ortiz, J. Cioslowski and D. J. Fox, *Gaussian 09, revision C.01*, Gaussian, Inc., Wallingford, CT, 2010.

S5 Ch. Baerlocher and L. B. McCusker, Database of Zeolite Structures. http://www.iza-structure.org/databases/.

S6 K.-P. Schröder, J. Sauer, M. Leslie, C. R. A. Catlow and J. M. Thomas, *Chem. Phys. Lett.*, 1992, **188**, 320.

S7 J. D. Gale and A. L. Rohl, *Mol. Simul.*, 2003, **29**, 291.

S8 S. L. Mayo, B. D. Olafson and W. A. Goddard, *J. Phys. Chem.*, 1990, **94**, 8897-8909.

S9 A. Rojas and M. A. Camblor, *Chem. Mater.*, 2014, **26**, 1161.

Table S1 Representative products from pure-silica zeolite syntheses at different temperatures using a series of imidazolium and pyrazolium derivatives as OSDAs

	Product[b]			Product	
	Crystallization conditions (*T*/*t*, °C/days)			Crystallization conditions (*T*/*t*, °C/days)	
OSDA[a]	125/21	175/14	OSDA	125/21	175/14
123TMI	ITW	ITW	123TMP	ITW	ITW
134TMI	ITW	ITW	124TMP	TON + MFI	TON + NON + MFI
1234TMI	STW	STW	1235TMP	STW	STW
1E23DMI	Amorphous	ITW	1E23DMP	ITW	ITW
2E13DMI	Amorphous	ITW	1E25DMP	Amorphous	NON
2E134TMI	STW	STW	1E235TMP	STW	HPM-2[c]

[a] The composition of the synthesis mixture is $0.50ROH \cdot 0.50HF \cdot 1.0SiO_2 \cdot 5.0H_2O$, where R is OSDA, and the abbreviations are the same as those in Fig. 1. All syntheses were performed under rotation (60 rpm). [b] The product appearing first is the major phase. [c] A layered precursor of zeolite MTF.

Table S2 Representative products from pure-silica zeolite syntheses at different H_2O/SiO_2 ratios using a series of imidazolium and pyrazolium derivatives as OSDAs

	Product[b]					Product			
	H_2O/SiO_2 ratio in the synthesis mixture					H_2O/SiO_2 ratio in the synthesis mixture			
	5.0	15.0				5.0	15.0		
OSDA[a]	14 days	3 days	7 days	14 days	OSDA	14 days	3 days	7 days	14 days
123TMI	ITW	ITW + A	ITW	ITW	123TMP	ITW	ITW + A	ITW	ITW
134TMI	ITW	A + TON	D	D	124TMP	TON + NON + MFI[c]	TON	TON + D	D
1234TMI	STW	A	A	ITW + D	1235TMP	STW	A	MTW + A	D
1E23DMI	ITW	MTW + A	MTW	MTW + D	1E23DMP	ITW	MTW + A	MTW	D + (MTW)
2E13DMI	ITW	A	MTW + A	MTW	1E25DMP	NON	A	A	D
2E134TMI	STW	A	A	STO* + D	1E235TMP	HPM-2[d]	A	STO* + A	D

[a] The composition of the synthesis mixture is $0.50ROH \cdot 0.50HF \cdot 1.0SiO_2 \cdot xH_2O$, where R is OSDA, and the abbreviations are the same as those in Fig. 1. All syntheses were performed under rotation (60 rpm) at 175 °C. [b] The product appearing first is the major phase, and the product obtained in a trace amount is given in parentheses. A and D indicate amorphous and dense phases, respectively. [c] The product obtained after 3 days of heating was the same. [d] A layered precursor of zeolite MTF.

Table S3 Chemical composition data for as-made crystalline products synthesized using imidazolium- and pyrazolium-based OSDAs with both methyl and ethyl groups

Sample[a]	TG[b] (wt %)	Weight found[d] (wt %)			Unit cell composition	No. of cavity per unit cell
		C	H	N		
1E23DMI-ITW	83.5				$\|(C_7H_{13}N_2F)_{2.0}(H_2O)_{0.2}\|[Si_{24}O_{48}]$[e,f]	2
2E13DMI-ITW	84.0				$\|(C_7H_{13}N_2F)_{1.9}(H_2O)_{0.4}\|[Si_{24}O_{48}]$[e,f]	2
2E134TMI-STW	79.9				$\|(C_8H_{15}N_2F)_{5.6}(H_2O)_{1.0}\|[Si_{60}O_{120}]$[e,f]	6
1E23DMP-ITW	83.8				$\|(C_7H_{13}N_2F)_{1.9}(H_2O)_{0.2}\|[Si_{24}O_{48}]$[e,f]	2
1E25DMP-NON	-[c]	4.57	1.14	1.53	$\|(C_7H_{13}N_2F)_{3.3}(H_2O)_{12.6}\|[Si_{88}O_{176}]$[g,h]	4
1E235TMP-HPM-2	81.0	10.54	1.97	2.90	$\|(C_8H_{15}N_2)_{3.4}(H_2O)_{6.6}\|[Si_{44}O_{88}]$[f,g,i]	-[j]

[a] The crystallization temperature and H_2O/SiO_2 ratio in the synthesis mixture employed were 175 °C and 5.0, respectively. [b] Residue in the thermogravimetric analysis up to 800 °C. [c] Cannot be accurately measured due to the non-porosity. [d] Determined from the CHN analysis. [e] The contents of H_2O and OSDAs and charge-compensating F^- anions were calculated from the weight loss by TGA/DTA up to 250 °C and 800 °C, respectively. [f] The SiO_2 content was calculated from the TG residue. [g] The OSDA content was calculated from the N analysis, assuming that the OSDA molecules remain intact, and the H_2O content was calculated from H excess *vs.* N. [h] The residue except H_2O, OSDAs, and F^- was assumed to be SiO_2. [i] The F^- content in this layered sample was neglected, due to the reason described in Ref. S9, and its unit cell composition was referenced on that of MTF zeolite. The H_2O content includes both water content and charge-compensating connectivity defects. [j] There are no cavies in layered HPM-2.

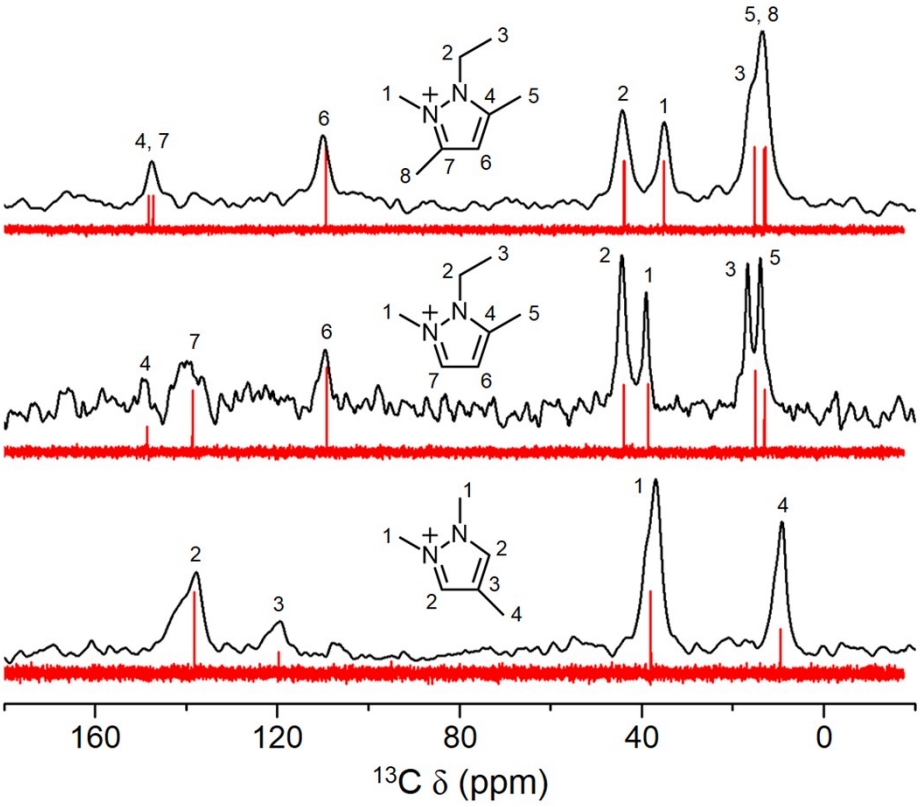

Fig. S1 ^{1}H-^{13}C CP MAS NMR spectra (black) of as-made pure-silica products (from bottom to top; TON + NON + MFI, NON, and HPM-2) using 124TMP, 1E25DMP, and 1E235TMP as an OSDA, respectively. The crystallization temperature and H_2O/SiO_2 ratio in the synthesis mixture employed were 175 °C and 5.0, respectively. The solution ^{13}C NMR spectra in D_2O (red) of the iodide salt of 124TMP, 1E25DMP, and 1E235TMP are also given for comparison.

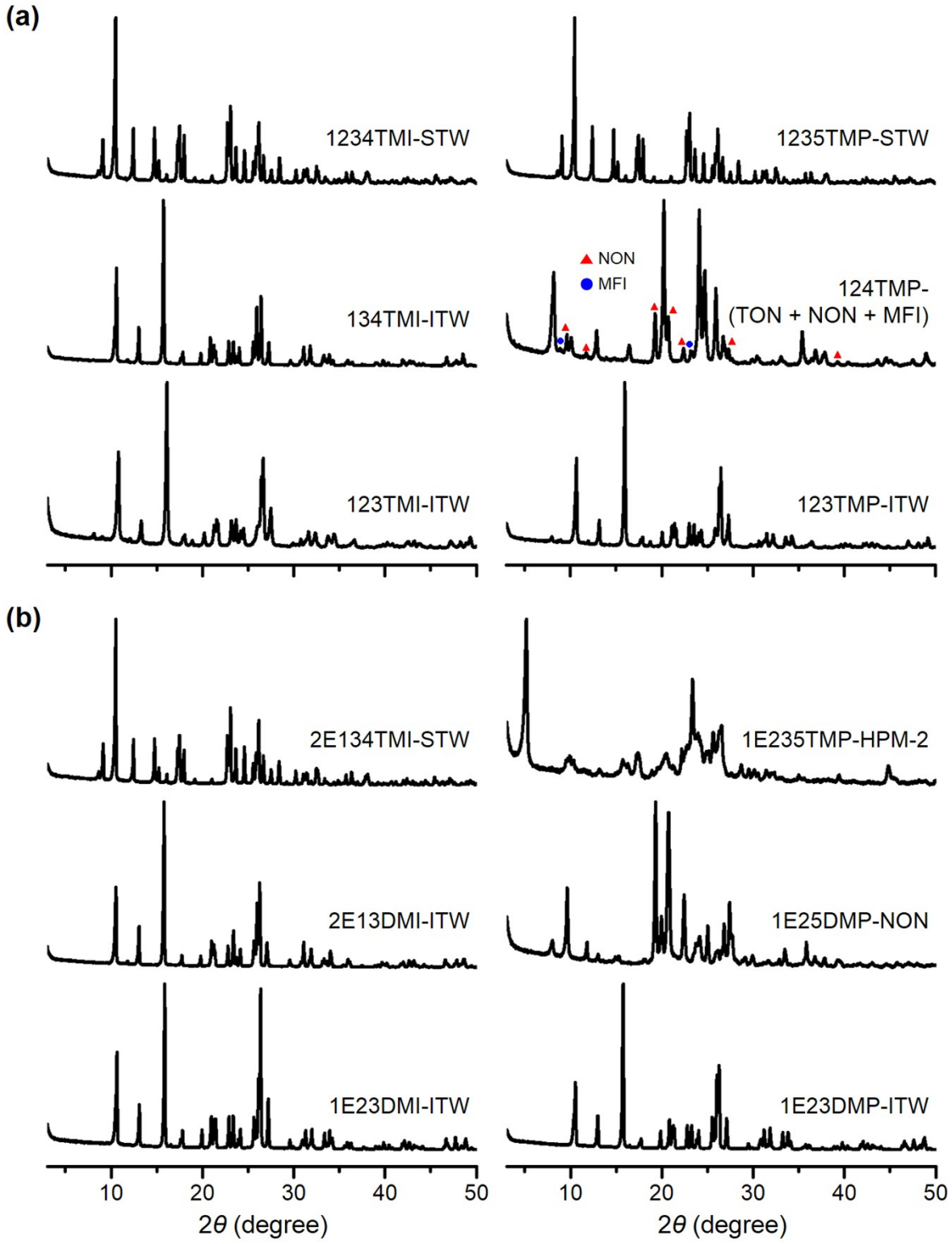

Fig. S2 Powder XRD patterns of as-made products synthesized using imidazolium- and pyrazolium-based OSDAs with (a) only methyl groups and with (b) both methyl and ethyl groups in fluoride media. The crystallization temperature and H_2O/SiO_2 ratio in the synthesis mixture employed were 175 °C and 5.0, respectively.

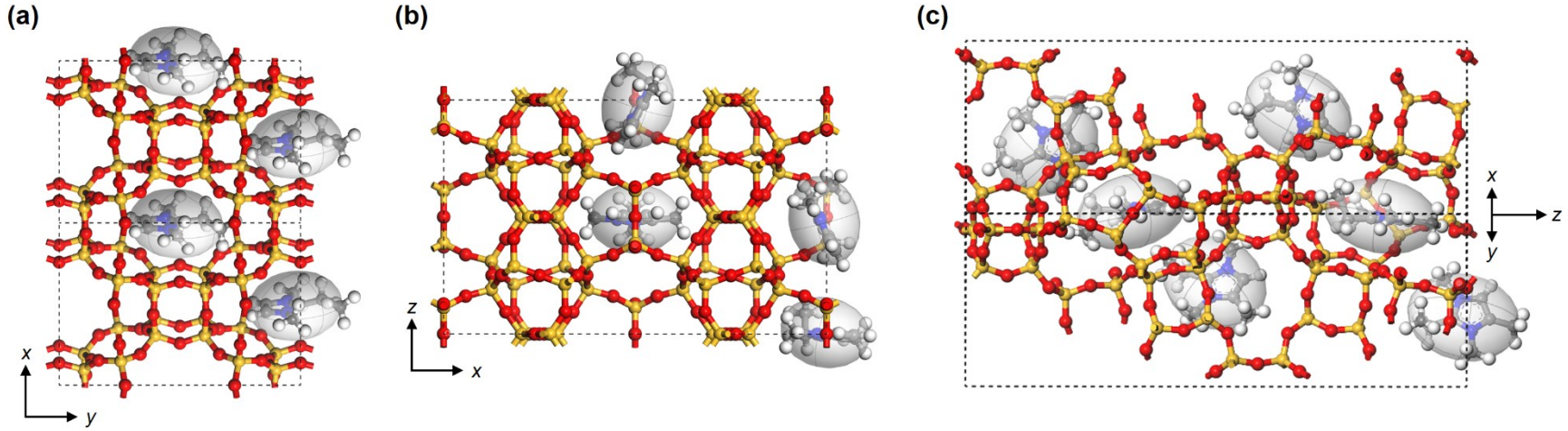

Fig. S3 (a) ITW, (b) NON, and (c) STW structures containing two 2E13DMI, four 1E25DMP, and six 2E134TMI cations per unit cell, respectively. The geometry of occluded OSDA molecules was optimized using the Dreiding potential. Si, yellow; O, red; C, grey; N, blue; H. white.

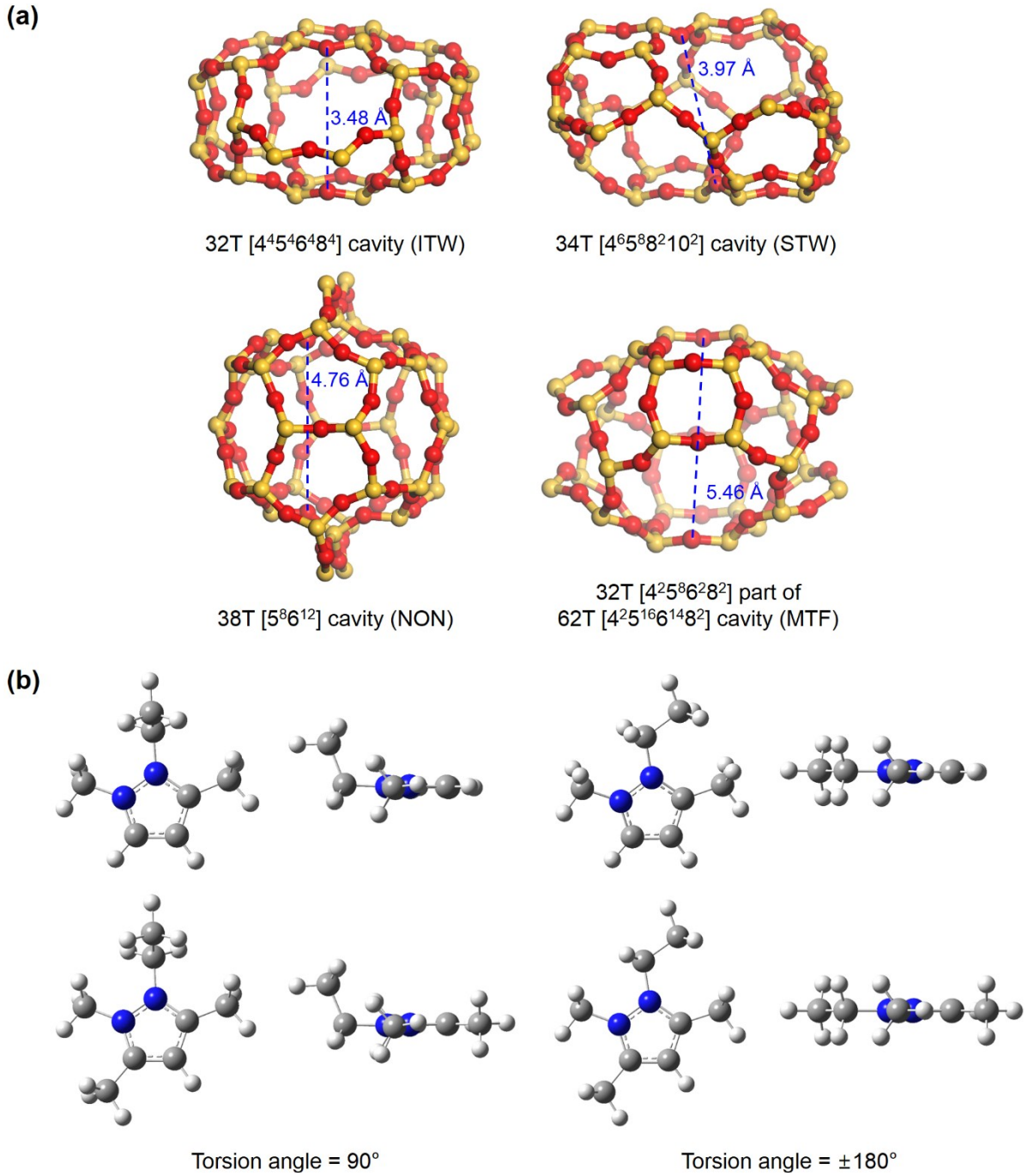

Fig. S4 (a) Cavities in the SLC-optimized ITW, STW, NON, and MTF structures. The O-O bond lengths marked here were calculated on the assumption that the radii of O atom is 1.52 Å. (b) Top and side views of 1E25DMP (upper) and 1E235TMP (bottom) optimized at the B3LYP/6-31+G(d,p) level when the $E_{Ar}(1)$-$E_{Ar}(2)$-$C_{Et}(3)$-$C_{Et}(4)$ torsion angles are fixed to 90 and ±180°, respectively. Si, yellow; O, red; C, grey; N, blue; H. white.

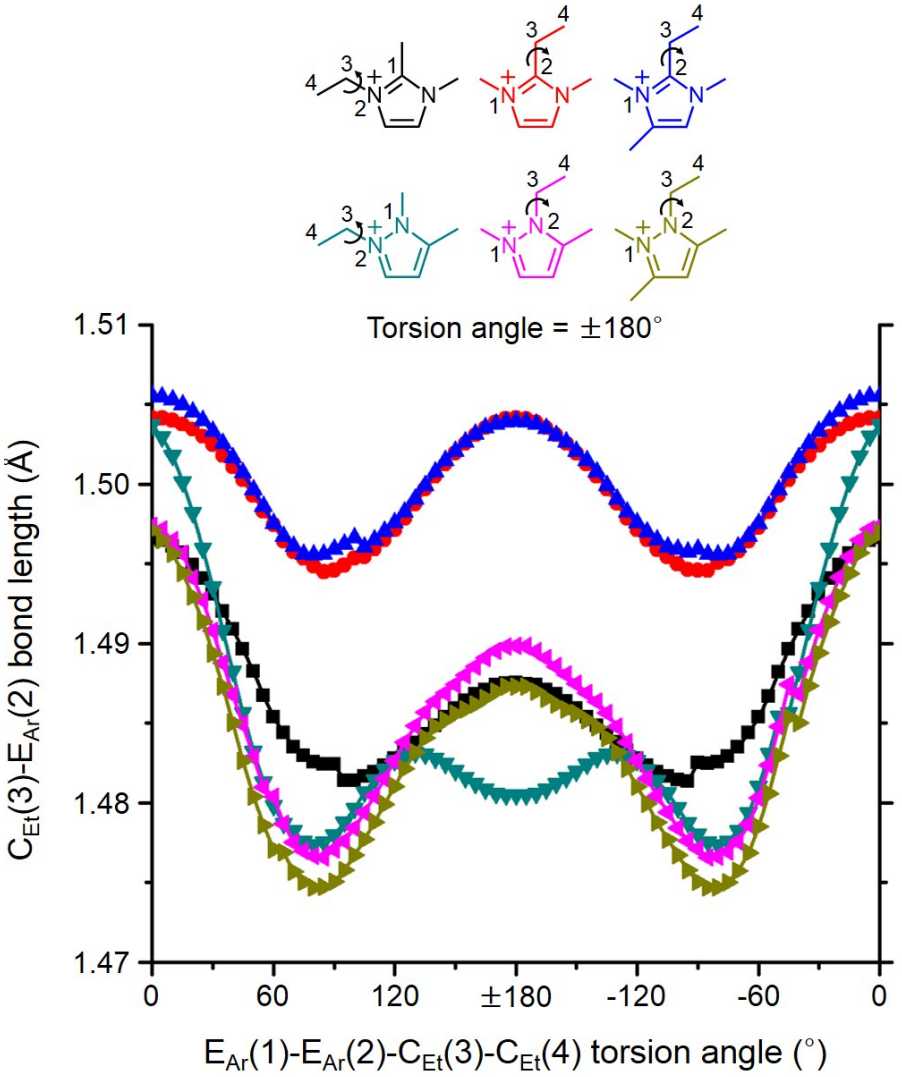

Fig. S5 $C_{Et}(3)$-$E_{Ar}(2)$ bond lengths scanned at the B3LYP/6-31+G(d,p) level of imidazolium- and pyrazolium-based OSDAs containing both methyl and ethyl groups as a function of $E_{Ar}(1)$-$E_{Ar}(2)$-$C_{Et}(3)$-$C_{Et}(4)$ torsion angle, where E is C or N.

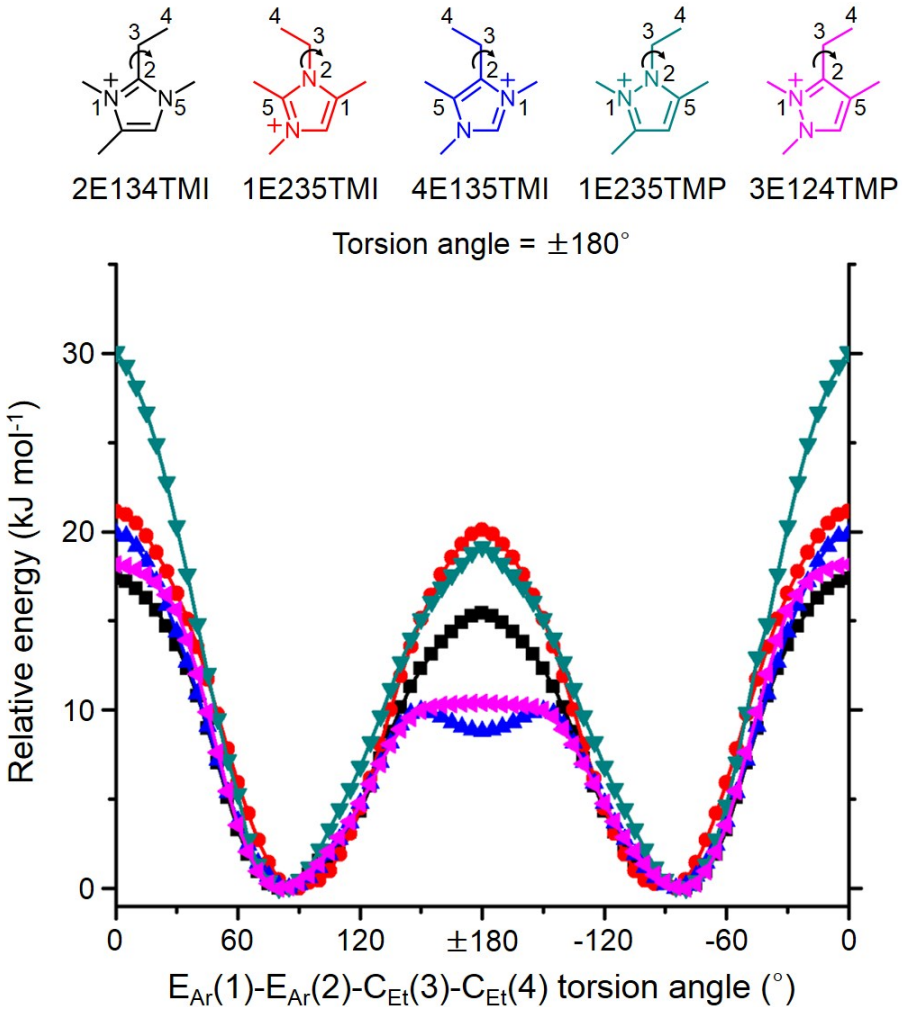

Fig. S6 Relative energies of five imidazolium and pyrazolium derivatives containing one ethyl and three methyl groups calculated at the B3LYP/6-31+G(d,p) level as a function of $E_{Ar}(1)$-$E_{Ar}(2)$-$C_{Et}(3)$-$C_{Et}(4)$ torsion angle, where E is C or N.